A Novel Equivalent Continuous Metering Control with a Uniform Switching Strategy for Digital Valve System

Pei Wang, Yuwang Cheng, Matti Linjama, Jing Yao* and Dongsheng Shan

***Abstract*—Pulse number modulation (PNM) combined with pulse width modulation (PWM) control is an effective solution to improve the resolution of digital valve systems. However, the numerous discrete variables that use parallel on/off valves cause difficult control coordination and uneven switching. To address this issue, this paper defines the equivalent spool displacement of the digital flow control unit (DFCU) by the number of PNM-controlled valves and the duty cycle of PWM-controlled valves to replace multiple discrete variables and develops the equivalent continuous metering control method. Furtherly, a uniform switching control strategy is proposed for the PWM-controlled valve using a uniformly distributed permutation for each on/off valve. The proposed control methods are verified by simulation on the built mathematical model of the equal-coded digital valve system. Experimental results for the displacement control of a hydraulic cylinder at 1 rad/s show that the average error of the equivalent continuous metering control is about 0.236 mm and the dispersion index reaches 20%, while the uniform switching control strategy achieves 80% with an average error of 0.215 mm. Simulated and experimental results demonstrate that the equivalent continuous metering control with a uniform switching strategy can almost evenly distribute switching numbers without compromising the accuracy of the displacement control.**

***Index Terms*—digital hydraulic, equal-code DFCU, independent metering, PNM, PWM, uniform switching**

I. Introduction

MOTION control technologies in industrial applications raised increasingly higher requirements for hydraulic transmission in terms of energy efficiency, controllability, cost, and reliability [1]. However, the high-end proportional/servo valves have a complex structure, poor efficiency, sensitivity to contamination, and high cost, which hinder the development of advanced control hydraulic systems [2-3]. Due to the benefits of energy savings, fault tolerance, strong interchangeability, cost-effectiveness, and reliability, digital hydraulics have become the forerunner and hotspot of modern fluid power technology [4-8], and are already applied in wind turbines, mobile cranes, aircraft braking system, etc. [9-15]. However, how to strike a balance between discrete variables, resolution or control accuracy, and reliability is a crucial problem for digital hydraulic systems.

DFCUs are the core control unit of digital hydraulics which provide an alternative to replacing proportional or servo valve-controlled systems with multiple discrete variables [16]. Binary-coded DFCUs can achieve higher resolution with fewer on/off valves, but there is no redundancy combinations and inconsistency of dynamic characteristics due to different specifications would cause output uncertainty such as pressure fluctuations; Fibonacci-coded DFCUs can alleviate the pressure fluctuations, which are the compromise between the number of on/off valves and the pressure fluctuations with the same resolution; Equal-coded DFCUs are ideal with high redundancy and reliability and no pressure fluctuations in theory. However, it faces the challenge of requiring a greater number of identical valves to achieve the higher resolution [17-19]. Pulse code modulation (PCM) or PNM are commonly used to control binary-coded or equal-coded DFCUs. But a relatively large number of valves are required for the equal-coded DFCU to generate high resolution [20]. While the PWM only uses one on/off valve with a variable pulse width and constant switching frequency as the input, resulting in severe wear, pressure fluctuations, noise, etc. [21-23]. Therefore, it makes sense to combine the PCM and PWM to reduce the number of valves and run part of them in the PWM mode to achieve high resolution [24]. Ferraresi studied the use of nine parallel on/off valves in a pneumatic system, one of which was driven with PWM at high frequency for fine-tuning and all others were used to compensate the step flow, resulting in wearing inconsistency among several valves [25, 26]. Huova et al. built a near binary-coded digital hydraulic system with four control edges, and the two smallest valves of each DFCU improved the output flow resolution by using the PWM [27]. Paloniitty et al. utilized multi-valve pulse frequency modulation (MPFM) and

Manuscript received Month xx, 2xxx; revised Month xx, xxxx; accepted Month x, xxxx. This work was supported by the National Natural Science Foundation of China under Grant 51975507 and the Innovation Funding for Postgraduates in Hebei Province under Grant CXZZBS2022141. *(Corresponding author: J. Yao).*

P. Wang, J. Yao and Y. Cheng are with the School of Mechanical Engineering, Yanshan University, and J. Yao is also with Hebei Provincial Key Laboratory of Heavy Fluid Power Transmission and Control, and Advanced Manufacture Forming Technology and Equipment, Qinhuangdao, 066004, China (e-mail: wangpeiysu@outook.com; jyao@ysu.edu.cn, +8613091368419; 593697592@qq.com).

M. Linjama is with Faculty of Engineering and Natural Sciences, Tampere University, Tampere 33720, Finland (e-mail: matti.linjama@tuni.fi).

D. Shan is with Ningbo Safe Brakes Systems Co., Ltd., Ningbo 315121, China (e-mail: sds@mail.tsinghua.edu.cn).

developed a circular buffered switching control in an equal-coded digital hydraulic system to achieve high resolution and linearity while causing pressure fluctuations and increasing switching numbers [28]. Gao et al. proposed a model-based PNM and a differential PWM controller for different working conditions to improve the low-speed control accuracy and designed a circular buffer for switching distribution, but it was complicated and consumed more energy [29, 30]. Most of the previous research has focused on model-based control methods that use PNM, PCM, PWM, or PFM to search for the optimal combination for multiple discrete variables. Furthermore, the huge difference in switching numbers between each valve will shorten its lifetime and significantly increase the cost of its maintenance [31].

Therefore, the following are the contributions of the paper: a) To overcome the difficulty of coordinated control among discrete variables, the equivalent spool under PNM and PWM compound control is defined for model-free continuous metering control of the equal-coded digital valve system (EDVS). Based on this, b) a uniform switching strategy based on uniformly distributed random permutations is proposed to evenly distribute the PWM-controlled valve, thereby improving overall system lifetime and reliability.

II. Modeling of Equal-coded Digital Valve System

A. Fitting Flow Model of the High-Speed Valve

A high-speed on/off valve (HSV) is the fundamental cell of DFCUs, the performance of which determines the output flow of DFCUs. The structure of HSVs from Ningbo Safe Brakes Systems Company is shown in Figure 1. Its max pressure is 24 MPa and nominal flow is 0.8 L/min@4MPa with around 3 ms response time. Four DFCUs, each with five identical HSVs connected in parallel, can be used to implement independent metering control in this paper.

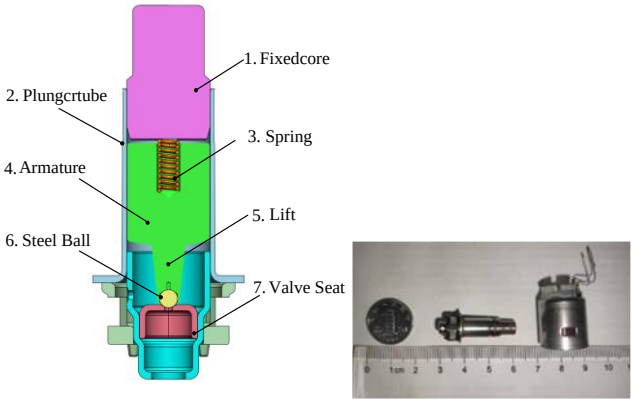

Fig. 1. The structure of the HSV

The steady-state HSV flow equations under the PNM and PWM control modes are as follow [32,33]:

$$q_{\mathrm{PNM}} = u(t)K_{\mathrm{v}}\Delta p^{m} \tag{1}$$

$$q_{\mathrm{PWM}} = \tau(t)K_{\mathrm{v}}\Delta p^{m} \tag{2}$$

where u(t) and τ(t) are the on/off signals and duty cycle signal, and the value is 0/1 or from 0 to 1, respectively; K_{v} denotes flow coefficient, Δp is the pressure difference between upstream and downstream pressure of the HSV, and m is the correction factor.

To obtain the flow coefficient K_{v} and correction factor m for an accurate mathematical model, the static characteristics (q-τ-Δp) of the HSV were conducted on the test bench, shown in Figure 2 (a). The pump can produce flowrate of 10 L/min, and the maximum pressure of pump outlet is 15 MPa. The measurable range of flow sensor is 0.01-10 L/min with ±0.05%FS used for monitoring the flowrate of the tested HSV. The relief valve adjusts the upstream pressure of the tested HSV from 1 MPa to 15 MPa in 1 MPa intervals and the downstream connects to the tank. Meanwhile, the PWM signal at 10 Hz is given to the HSV, and the duty cycle τ gradually increases from 0 to 1 with a gradient of 0.05 at each adjusted pressure. The test result is shown in Figure 2 (b).

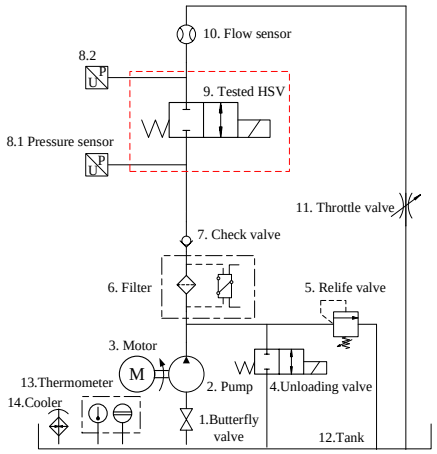

(a) Schematic of the test circuit

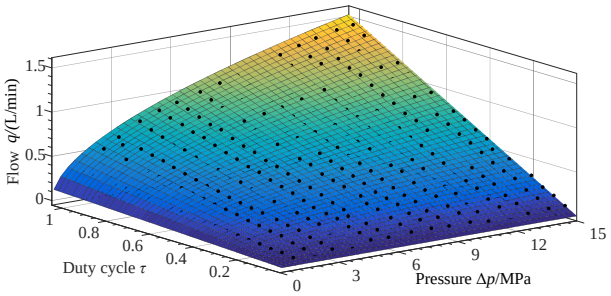

(b) q-τ-Δp and fitting curves

Fig. 2. Measured static characteristics of the HSV

The flow coefficient K_{v} is considered a constant value in this study. The mathematical model of HSV is highly fitted in the MATLAB toolbox by tested data, then K_{v}=0.3658 and m=0.5084 are obtained. Therefore, the fitting flow model can be rewritten by Eqs. (3)-(4):

$$q_{\mathrm{PNM}} = u(t)\cdot 0.3658\cdot \Delta p^{0.5084} \tag{3}$$

$$q_{\mathrm{PWM}} = \tau(t)\cdot 0.3658\cdot \Delta p^{0.5084} \tag{4}$$

Equation (3) and (4) describe the precise mathematical model of the steady-state flow of HSV. The coefficient of determination (R-square) is 0.996, and the sum of squares due to error (SSE) is 0.124 (L/min) ^{2} and root mean squared error (RMSE) is 0.02064 L/min.

B. Flow Equation of the DFCU

It is assumed that the DFCU is composed of *a* HSVs controlled by the PNM signal and *b* HSVs controlled by the PWM signal. Referring to [34,35], the flow calculation model under the PNM and PWM compound control can be expressed by Eq. (5):

$$Q = Q_{\mathrm{PNM}} + Q_{\mathrm{PWM}} = \sum_{i=1}^{a} K_{vi} u_i \Delta p^m + \sum_{j=1}^{b} K_{vj} \tau_j \Delta p^m \tag{5}$$

The opening of the equal-coded DFCU is equivalent to the spool displacement of a proportional valve to achieve the approximately continuous flow output. The opening numbers of the PNM together with the duty cycle of the PWM is defined as the opening of DFCU, that is the equivalent spool displacement x_v ($x_v \in [0,1]$, $u_i \in \{0,1\}$, $\tau_j \in \{0.01, 0.02, \ldots, 0.99, 1\}$) which can be solved by Eq. (6):

$$\begin{cases} Q = K_v(\sum_{i=1}^{a} u_i + \sum_{j=1}^{b} \tau_j)\Delta p^m = \bar{K}_v \cdot x_v \cdot \Delta p^m \\ \bar{K}_v = (a+b)K_v \\ x_v = \dfrac{\sum_{i=1}^{a} u_i + \sum_{j=1}^{b} \tau_j}{a+b} \end{cases} \tag{6}$$

where $\bar{K}_v$ is the equivalent flow coefficient of the DFCU.

For example, Figure 3(a) depicts the 5-bit equal-coded DFCU with four PNM-controlled HSVs and one PWM-controlled HSV in this study.

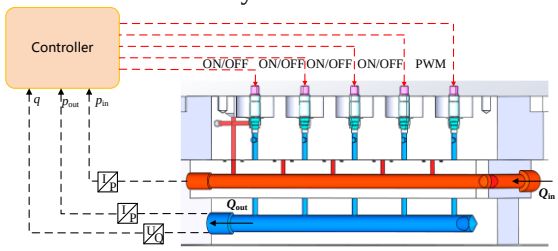

(a) PNM combined PWM control mode

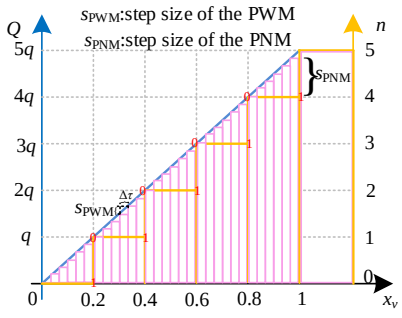

(b) Mapping relationships between Q, x_v, n and τ

Fig. 3. Equal-coded DFCU and equivalent spool displacement

In Figure 3(b), the equivalent spool displacement $x_v \in [0,1]$ can be divided into five parts equally, and each valve represents 0.2 for one part according to Eq. (6). The blue and yellow lines represent the reference flow Q and the flow of the PNM-controlled valves, respectively. The rest part of the flow can be compensated by the calculated duty cycle of a PWM-controlled valve by pink stripes. Clearly, a higher resolution can be obtained by dividing the duty cycle of a PWM-controlled valve into more parts, approaching a continuous spool displacement.

According to the flow range of Q, the equivalent spool displacement can be expressed as Eqs. (7)-(11). If $Q \in [0,q)$, a single PWM-controlled valve can meet flow requirement. The spool displacement x_v belongs to [0, 0.2), written as Eq. (7):

$$0 \le Q < q, 0 \le x_v < 0.2, x_v = \frac{\tau}{5} = \frac{Q}{5K_v\Delta p^m}; \tag{7}$$

If $Q \in [q,2q)$, the flow is provided by a PNM-controlled valve and a PWM-controlled valve. The spool displacement x_v belongs to [0.2, 0.4), and the value of x_v is written by Eq. (8):

$$q \le Q < 2q, 0.2 \le x_v < 0.4, x_v = 0.2 + \frac{\tau}{5} = 0.2 + \frac{Q-q}{5K_v\Delta p^m}; \tag{8}$$

Similarly, the x_v can be expressed as Eqs. (9)-(11) for different flow ranges:

$$2q \le Q < 3q, 0.4 \le x_v < 0.6, x_v = 0.4 + \frac{\tau}{5} = 0.4 + \frac{Q-2q}{5K_v\Delta p^m}; \tag{9}$$

$$3q \le Q < 4q, 0.6 \le x_v < 0.8, x_v = 0.6 + \frac{\tau}{5} = 0.6 + \frac{Q-3q}{5K_v\Delta p^m}; \tag{10}$$

$$4q \le Q < 5q, 0.8 \le x_v < 1, x_v = 0.8 + \frac{\tau}{5} = 0.8 + \frac{Q-4q}{5K_v\Delta p^m}; \tag{11}$$

C. Modelling of the Equal-coded Digital Valve System

The schematic diagram of the EDVS composed of four equal-coded DFCUs is shown in Figure 4.

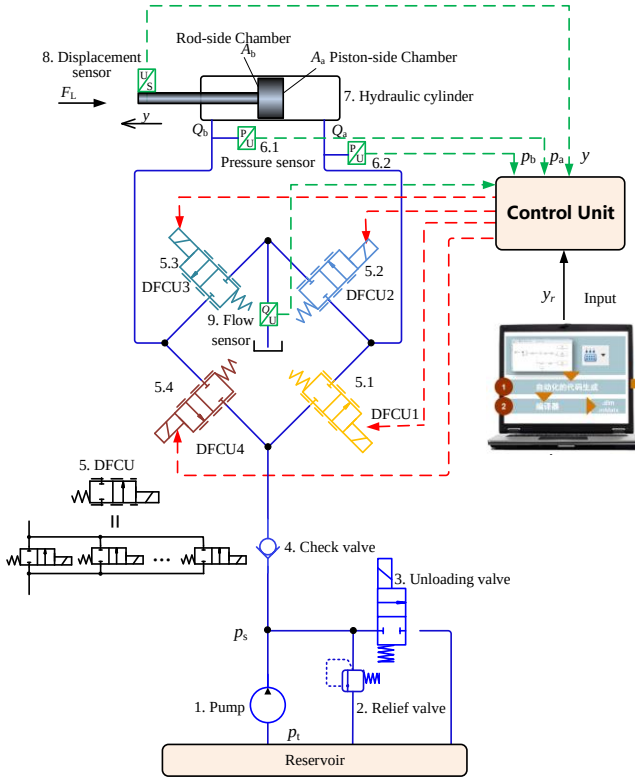

Fig. 4. A schematic view of the EDVS

Combined with Eq. (5), the flow equation of four DFCUs can be written by Eq. (12):

$$\begin{cases} Q_1 = \bar{K}_{v1} \cdot x_{v1} \cdot (p_s - p_a)^m, \\ Q_2 = \bar{K}_{v2} \cdot x_{v2} \cdot (p_a - p_t)^m, \\ Q_3 = \bar{K}_{v3} \cdot x_{v3} \cdot (p_b - p_t)^m, \\ Q_4 = \bar{K}_{v4} \cdot x_{v4} \cdot (p_s - p_b)^m, \end{cases} \tag{12}$$

where Q_1, Q_2, Q_3 and Q_4 are the flow of corresponding DFCUs; p_a, p_b, p_s, and p_t are the piston-side and rod-side pressure of the cylinder, and the supply and tank pressure, respectively.

The flow equations of the piston-side and rod-side chamber of the hydraulic cylinder for the extension and retraction are expressed by Eq. (13)-(14):

$$\begin{cases} Q_a = Q_1, \\ Q_b = Q_3, \end{cases} \tag{13}$$

$$\begin{cases} Q_a = Q_2, \\ Q_b = Q_4, \end{cases} \tag{14}$$

The compressibility of the hydraulic fluid is considered in the model. The bulk modulus of the hydraulic fluid is represented by β and it is assumed to be constant. However, the compliance effect of the actuator is neglected. Also, the pipelines are assumed to be rigid and the volume of the fluid between the valve and actuator is small since the valve is very close to the actuator. Hence, the flow continuity equations for both chambers of the hydraulic actuator are given by Eq. (15)-(16):

$$Q_a = A_a \frac{\mathrm{d}y}{\mathrm{d}t} + C_{ip}(p_a - p_b) + C_{ep} p_a + \frac{V_a}{\beta} \frac{\mathrm{d}p_a}{\mathrm{d}t} \tag{15}$$

$$Q_b = A_b \frac{\mathrm{d}y}{\mathrm{d}t} + C_{ip}(p_a - p_b) - C_{ep} p_b - \frac{V_b}{\beta} \frac{\mathrm{d}p_b}{\mathrm{d}t} \tag{16}$$

where y is the displacement of the hydraulic cylinder; C_{ip} and C_{ep} are the internal leakage and external leakage coefficient; $V_a = V_0 \pm A_a y$ and $V_b = V_0 \mp A_b y$, V_0 is the initial piston-side and rod-side volume of the hydraulic cylinder. V_a and V_b are the piston-side and rod-side volume, respectively.

The force balance of the system is given by Eq. (17):

$$A_a p_a - A_b p_b = M \frac{\mathrm{d}^2 y}{\mathrm{d}t^2} + B \frac{\mathrm{d}y}{\mathrm{d}t} + Ky + F_L \tag{17}$$

where M is equivalent mass, K is stiffness, B is viscous damping coefficient, F_L is load force.

III. Control Algorithms

A. Uniform switching strategy for the DFCU

The PWM-controlled valve switches at its frequency, and it would be more switching numbers and is easier to wear. Hence, the uniform switching strategy for the PWM-controlled valve of the DFCU is proposed to make the PWM control run to another valve randomly and evenly distribute the switching numbers of the DFCU, and it is described in Figure 5.

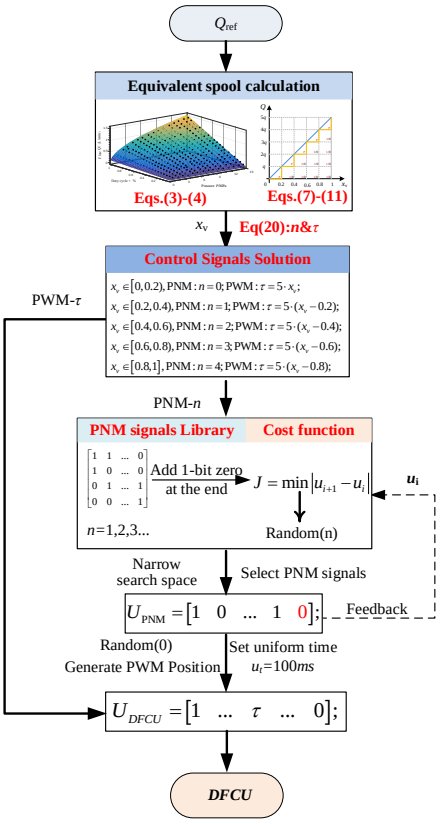

Fig. 5. Process of the uniform switching strategy for one DFCU

1) **Number and Duty cycle**

For flow control of one DFCU, the equivalent spool displacement x_v can be calculated by Equation (7)-(11) according to Q_{ref}. The opening number n of PNM-controlled valves and the duty cycle τ of PWM-controlled valve can be derived according to the following equation (18):

$$\begin{aligned} &x_v \in [0, 0.2), \mathrm{PNM}: n = 0; \mathrm{PWM}: \tau = 5 \cdot x_v; \\ &x_v \in [0.2, 0.4), \mathrm{PNM}: n = 1; \mathrm{PWM}: \tau = 5 \cdot (x_v - 0.2); \\ &x_v \in [0.4, 0.6), \mathrm{PNM}: n = 2; \mathrm{PWM}: \tau = 5 \cdot (x_v - 0.4); \\ &x_v \in [0.6, 0.8), \mathrm{PNM}: n = 3; \mathrm{PWM}: \tau = 5 \cdot (x_v - 0.6); \\ &x_v \in [0.8, 1], \mathrm{PNM}: n = 4; \mathrm{PWM}: \tau = 5 \cdot (x_v - 0.8); \end{aligned} \tag{18}$$

2) **Signal Subsets**

PNM signal subsets $U_{n=i}$ are established based on the opening number n of PNM-controlled valves by Eq. (19), such as $U_{n=0}$, $U_{n=1}$, $U_{n=2}$, $U_{n=3}$, $U_{n=4}$. The zero elements are added in the last row of the matrix for PWM-controlled valve.

$$U_{n=0} = \begin{bmatrix} 0 \\ 0 \\ 0 \\ 0 \\ 0 \end{bmatrix}; U_{n=1} = \begin{bmatrix} 1 & 0 & 0 & 0 \\ 0 & 1 & 0 & 0 \\ 0 & 0 & 1 & 0 \\ 0 & 0 & 0 & 1 \\ 0 & 0 & 0 & 0 \end{bmatrix}; U_{n=2} = \begin{bmatrix} 1 & 1 & 1 & 0 & 0 & 0 \\ 1 & 0 & 0 & 1 & 1 & 0 \\ 0 & 1 & 0 & 1 & 0 & 1 \\ 0 & 0 & 1 & 0 & 1 & 1 \\ 0 & 0 & 0 & 0 & 0 & 0 \end{bmatrix};$$
$$U_{n=3} = \begin{bmatrix} 1 & 1 & 1 & 0 \\ 1 & 1 & 0 & 1 \\ 1 & 0 & 1 & 1 \\ 0 & 1 & 1 & 1 \\ 0 & 0 & 0 & 0 \end{bmatrix}; U_{n=4} = \begin{bmatrix} 1 \\ 1 \\ 1 \\ 1 \\ 0 \end{bmatrix}; \tag{19}$$

Each column of the matrixes has five elements that represent the control signal of each HSV. The number of rows means the combination numbers of PNM-controlled valves under the its opening number n=i.

3) **Cost Function**

A cost function J is expressed by Eq. (20) to find the minimum switching numbers based on the PNM control signals of the previous sampling time ($\mathbf{u}_i$ is the previous PNM signal, and $\mathbf{u}_{i+1}$ is the current PNM signal):

$$J = \min\left|\mathbf{u}_{i+1} - \mathbf{u}_i\right| \tag{20}$$

4) **PNM Signals**

The combination(s) with minimum switching numbers were selected through the cost function, which represents PNM control signals. The Randperm function is utilized in MATLAB to randomly select one combination from a group of PNM control signals with same minimum switching numbers. Meanwhile, the selected PNM signal is fed back to the next cycle.

5) **Uniform Switching of PWM Signals**

The locations of the zero elements in the current control signal matrix are read. Randperm function is used once more to select one location from zero elements for the PWM control. Considering the switching frequency of the PWM-controlled valve, the changing cycle of the PWM location is set as u_t=100 ms, meaning that the PWM-controlled valve will be changed randomly every 100 ms.

6) **Signals Output**

The signals of PWM and PNM output to the HSVs and this strategy is applied to each DFCU. Hence, the switching numbers of each HSV in the DFCU are close, which avoids one of them switching very frequently.

In this paper, a normalized dispersion index D is written as Eq. (21). It is defined as the percentage that 1 subtracts the ratio that the sum of the squares of the switching numbers of each valve to the square of the total switching number of all on/off valves, which characterizes the degree of uniform switching of the DFCU.

$$D = (1 - \frac{\sum S^2}{(\sum S)^2}) \times 100\% \tag{21}$$

As mentioned above, the uniform switching strategy for the DFCU would be considered in the EDVS combined with the equivalent spool displacement to achieve the equivalent continuous metering control. As an illustration, Figure 6 depicts the meter-in with displacement control and meter-out with pressure control. For the closed-loop control of EDVS, the equivalent spool displacement x_v can be calculated by the error and controller, and the closed-loop PID controller converts the error e_y between target and actual displacement to the equivalent spool displacement x_v. The DFCU-PA for extension or PB for retraction would be selected depending on the positive or negative of the error e_y.

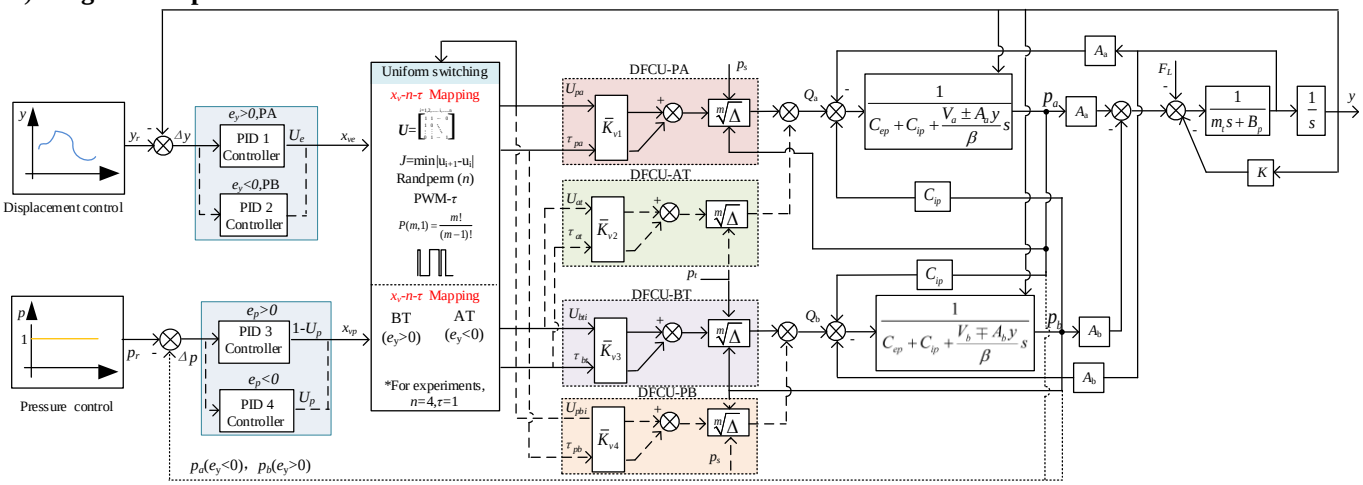

Fig. 6. Block diagram representation of the EDVS

Similarly, the x_v of DFCU-BT for extension or DFCU-AT for retraction is determined by the sign of error e_p between target and actual pressure ($e_p \geq 0$, $x_v = e_p$; $e_p < 0$, $x_v = 1 - e_p$). Then, Eq. (18) would be used to calculate the number n of opening PNM-controlled valves and the duty cycle τ of PWM-controlled valves in step 1). The uniform switching strategy is then implemented in DFCUs using steps 2)-6). Finally, the equivalent continuous metering control with a uniform switching strategy can come true.

B. Simulation verification

Based on the mathematical model in Section 2 and control algorithms in Section 3, A., the EDVS simulation model were built by MATLAB/Simulink to verify the feasibility and the effectiveness of the equivalent continuous metering control method and uniform switching strategy. The main parameters for it are listed in Table I.

TABLE I THE MAIN PARAMETERS OF THE SIMULATION

Element	Name	Specification
Hydraulic cylinder	Piston diameter D	70 mm
	Rod diameter d	50 mm
	Stroke l	200 mm
Others	Bulk modulus β	0.7×10^9 Pa
	Stiffness K	1×10^3 N/m
	Viscous damping coefficient B	5000 N/(m/s)
	Equivalent mass M	10 kg

It is assumed that the load in the hydraulic system is mainly inertial load, and the elastic load is small. The friction and leakage are ignored in this simulation case. The external load force F_L=6000sin(pi/8)t and reference displacement y=50+30sin(pi/8)t are given. System pressure p_s is set to 100 bar and tank pressure p_t is zero. The reference back pressure p_r is set to 10 bar. Figure 7-11 show the simulation results of the equivalent continuous metering control for the EDVS.

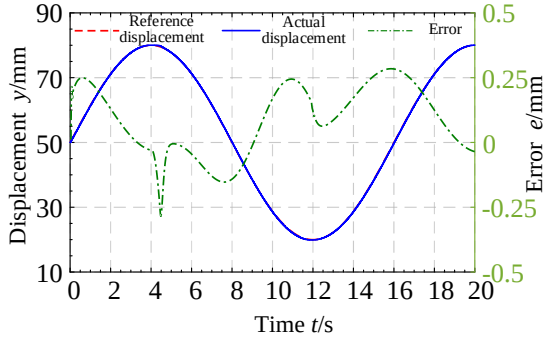

Fig. 7. Displacement and error curves

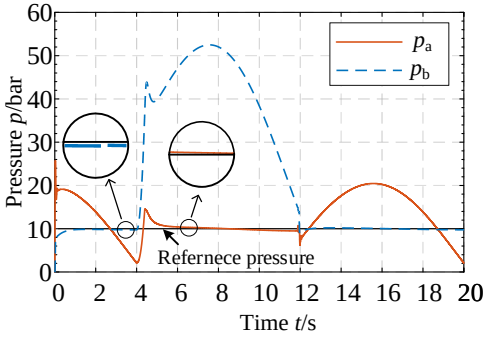

Fig. 8. Pressure curves

The maximum position error is about 0.27 mm under the equivalent continuous metering control. However, the back pressure would change from rod-side chamber p_b to the piston-side chamber p_a when the hydraulic cylinder moves from extending to retracting, resulting in pressure shock of about 6 bar. The back pressure is basically maintained at 10 bar and the control error $|p_r$-$p_b|$ or $|p_r$-$p_a|$ is within 0.01 bar. The low back pressure could reduce the throttling loss of tank side, and it is possible to save energy by decreasing the system input power p_s and it would be studied further.

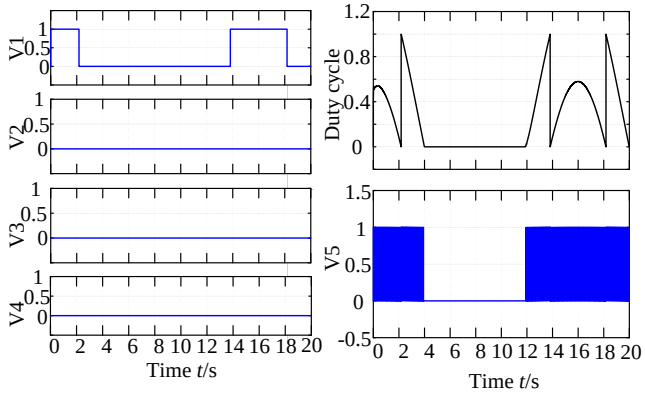

Fig. 9. Control signals of the DFCU-PA

As an example, Figure 9 shows DFCU-PA control signals. The PWM control acts on the HSV V5, while the other HSVs V1-V4 are controlled by the PNM. The switching numbers of HSV V5 is significantly more than that of the PNM-controlled valves, and V5 is more prone to wear failure.

Figures 10-11 show the simulation results of the equivalent continuous metering control under the uniform switching strategy for the EDVS. The position error varies from -0.3 to 0.4 mm with uncertain switching impact on the displacement control. The pressure is basically consistent compared to that of the non-uniform switching strategy. There is an effect on the back pressure chamber when reversing, with the control error of about 0.1 bar at 10 bar reference pressure. Figures 12-13 show that the duty cycle of each valve is superimposed together equal the theoretical duty cycle τ. The duty cycle is assigned to one valve every 100 ms and switching numbers are randomly distributed to five HSVs in the DFCU-PA.

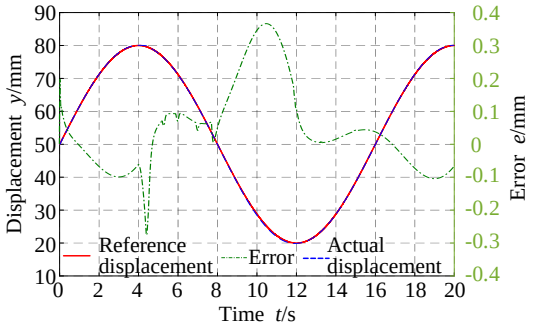

Fig. 10. Displacement and error curves

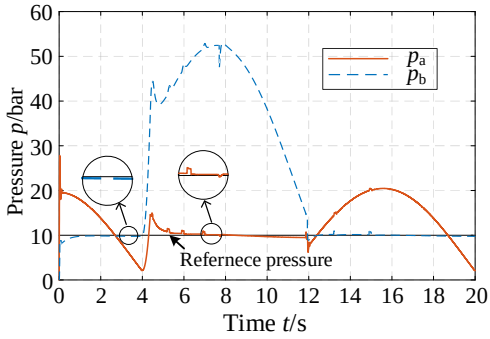

Fig. 11. Pressure curves

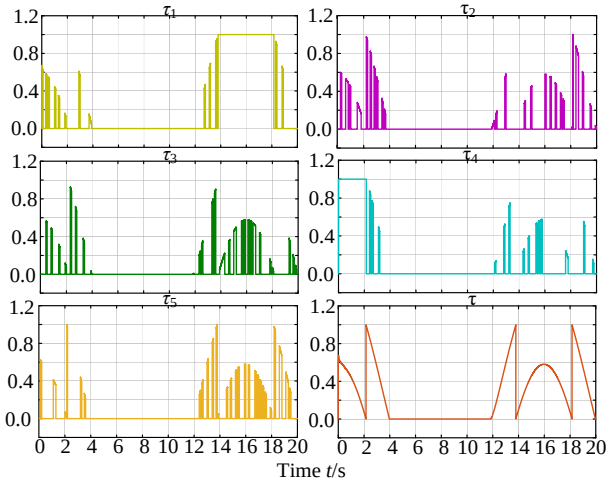

Fig. 12. Distribution of the duty cycle

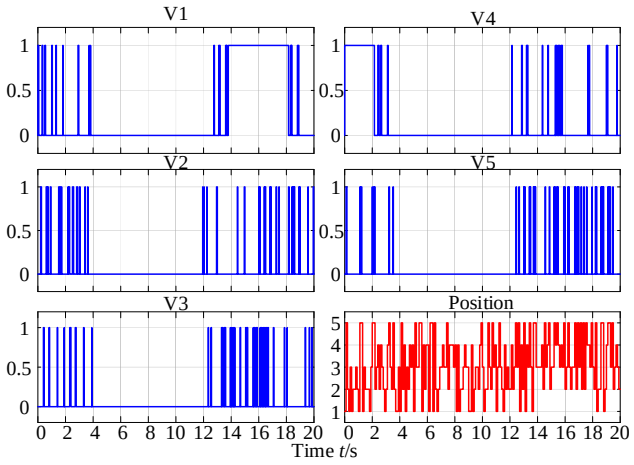

Fig. 13. Control signals of the DFCU-PA

The switching numbers of each valve in the DFCU-PA and their total switching numbers that are calculated under non-uniform switching and uniform switching, shown in Tables II.

TABLE II THE SWITCHING NUMBERS COMPARISON

Switching Number (S)	Non-uniform switching	Uniform switching
V1	3	38
V2	0	72
V3	0	76
V4	0	42
V5	241	88
Total	245	316
D	3.22%	78.06%

The dispersion indexes D of DFCU-PA with the uniform and non-uniform switching control strategies were 78.06 % and 3.22 %, respectively. Compared to the non-uniform switching strategy, the switching numbers increase slightly with the pressure fluctuation of about 0.1 MPa caused by alternating the PWM position, but the switching numbers of all valves are evenly distributed under the uniform switching strategy based on uniformly distributed random permutations. It can not only avoid the frequent switching influence of a single digital valve on the reliability of EDVS but also significantly reduce maintenance costs.

IV. RESULTS AND DISCUSSION

A. Experimental setup

An experimental setup is constructed for the design and development of the EDVS according to the above schematic view, shown in Figure 4. It mainly consists of (a) the load simulator with three parallel springs fixed to the test bench, (b) the DFCUs and hydraulic cylinder, (c) Rexroth oil source used for power supply, and (d) the data acquisition and control unit.

A baseline real-time target machine is equipped by Speedgoat IO 397 (FPGA Bitstream file) for PWM output at 10 Hz and Beckoff EL2809 and EL3124 modules for the analog input and digital output, which is as the data acquisition and control unit. To achieve real-time control of the EDVS, the MATLAB® R2020a software, as well as Simulink®, Real-Time Workshop®, and xPC Target™, are installed on the host PC. The equivalent continuous metering control and uniform switching control algorithms are designed in the MATLAB®/Simulink® environment, and the control program solver is a 4th order Runge-Kutta (ode4) with a fixed step of 1 ms. The control program is compiled in the host PC using a Visual C compiler and downloaded to the baseline real-time target machine via Ethernet communication. The main parameters are listed in Table III.

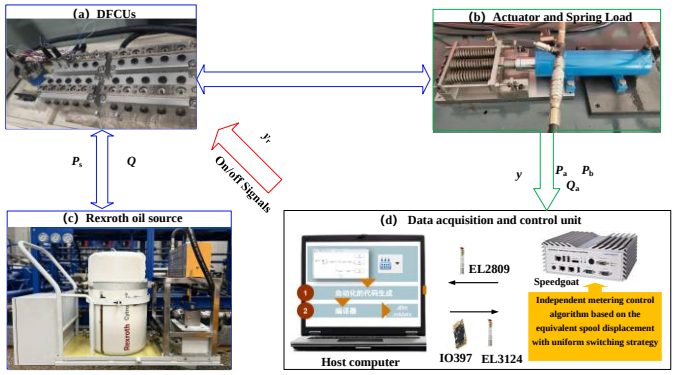

Fig. 14. Test bench of EDVS

TABLE III THE MAIN PARAMETERS OF THE SETUP

Element	Name	Specification
Flow sensor	Range	0.01~10L/min
	Accuracy	±0.05%FS
Pressure sensors	Range	0~60 MPa, 0~25 MPa,
	Accuracy	±0.25%FS
Displacement sensor	Range	0~1000 mm
	Linearity Accuracy	±0.1%FS
Hydraulic cylinder	Piston diameter	70 mm
	Rod diameter	50 mm
Load simulator	Stiffness K	3×24 N/mm
Rexroth pump	Nominal Pressure	24 MPa
	Nominal Flow	16 L/min
Air cooler	Maximum pressure	2 MPa
	Maximum flow	60L/min
Relief valve	Maximum pressure	31.5 MPa
	Maximum flow	40 L/min

B. Results analysis

The reference sine displacement y is given at ω_1=1rad/s and ω_2=1.5 rad/s, with the mean value and amplitude being 30 mm and 20 mm in those experiments, respectively. The elastic load is selected due to existing conditions, which is proportional to the displacement $F_L=Ky$, and the spring is in a compression state, allowing for resistant and assistant working quadrants. The system pressure p_s is set around 60 bar, and the tank comes with around 1 bar. So the full opening control with more energy-saving potential is adapted for the chamber of back pressure, and the displacement control is adopted by the other chamber for position control according to the sign of error e, as * for experiments shown in Figure 6. Different metering control modes for each DFCU in four quadrants that provide greater energy savings potential will be investigated by experiments in the future.

The model-free equivalent continuous metering control with or without a uniform switching can be validated and analyzed by the performance indicator $\rho=|e_{max}|/|v_{max}|$, which relatively reflects the performance of different control methods in a comparative manner [36,37].

*1) **Equivalent Continuous Metering Control***

Figure 15-16 show the average error is about 0.236 mm and the back pressure is around 1 bar. The calculated quality factor of the control system is 0.128 s by the maximum position error 0.831 mm to the maximum velocity 6.483 mm/s. The p_a changes with the load force varying with the displacement. The p_b is basically the same as the tank pressure, representing independent control and low throttling loss of the tank side. During the reversing from retraction to extension, the load force F_L decreases gradually in assistant condition during the retraction process, and the p_a decrease slowly to balance F_L. At 51-60 s, because F_L is insufficient to push the piston due to the gradually decreasing displacement, p_b suddenly rises along with the load force F_L to balance p_a.

Similarly, Figure 18 shows that the displacement tracks well with the reference displacement, but the error is slightly larger than at ω_1, where the average error is around 0.406 mm and the maximum error is 1.59 mm. The quality factor of this control method is 0.112 s, calculated by the maximum position error of 1.59 mm to the maximum velocity of 14.20 mm/s. It can be seen from Figure 17 and 19 the duty cycle is calculated in real-time through the control algorithm. The PWM control always acts on valve V1 and other valves are controlled by PNM with fewer switching numbers. The failure rate of valve V1 may increase significantly and simultaneously, which is not good for the overall reliability of the DFCUs.

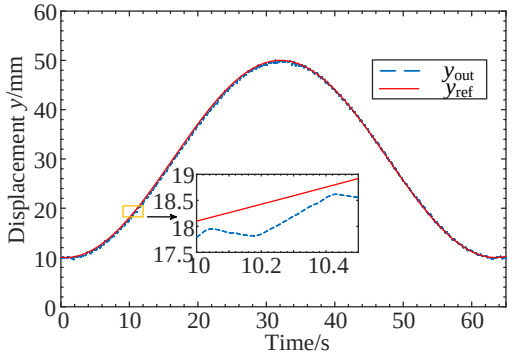

Fig. 15. Displacement curves at ω_1

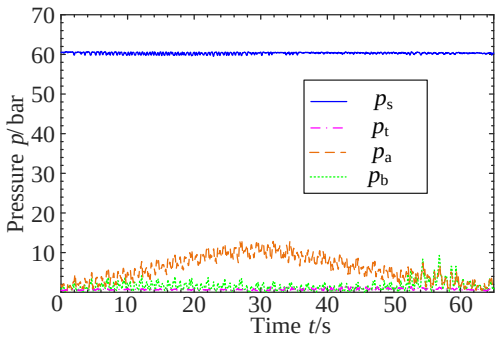

Fig. 16. Pressure curves at ω_1

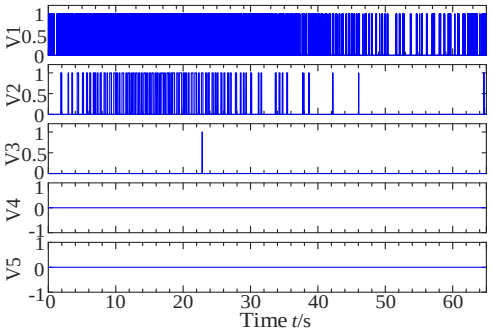

Fig. 17. Signals of PA-DFCU at ω_1

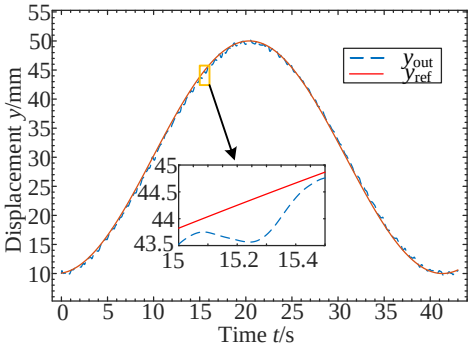

Fig. 18. Displacement curves at ω_2

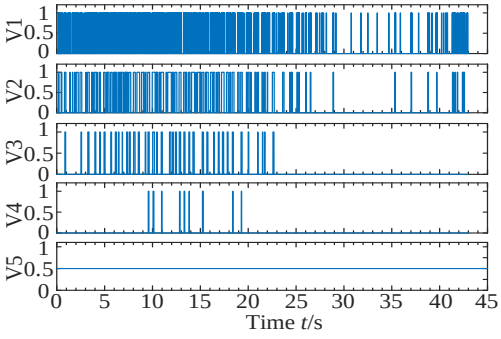

Fig. 19. Signals of PA-DFCU at ω_2

*2) **Equivalent Continuous Metering Control with Uniform Switching Strategy***

Figures 20–21 show that the average position control accuracy is around 0.215 mm, and which is close to the non-uniform switching strategy. The quality factor is around 0.14 s for the maximum position error of 0.830 mm to the maximum velocity of 5.943 mm/s. The change in pressure is also similar to the non-uniform switching, but there is minor pressure fluctuation during movement.

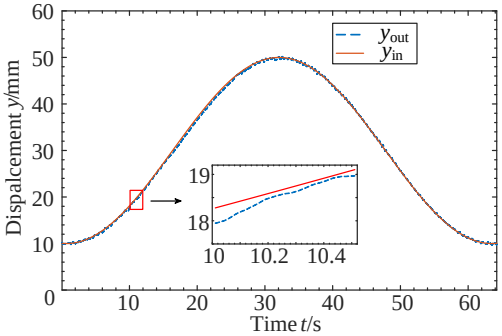

Fig. 20. Displacement curves at ω_1

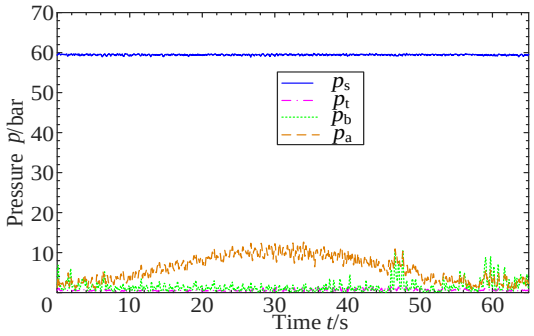

Fig. 21. Pressure curves at ω_1

Figure 22 depicts how changes in the duty cycle between 0 and 1 with the uniform switching control based on uniformly distributed random permutations. One HSV in the DFCU is randomly assigned a duty cycle for PWM control, and its position changes every 100ms. The duty cycle of each valve corresponds to its switch signal at 10Hz, and the sum of them is consistent with the theoretical duty cycle, demonstrating the effectiveness of the uniform switching control strategy. Each HSV signal is determined by the assigned duty cycle and the cost function of the uniform switching control strategy, as shown in Figure 23.

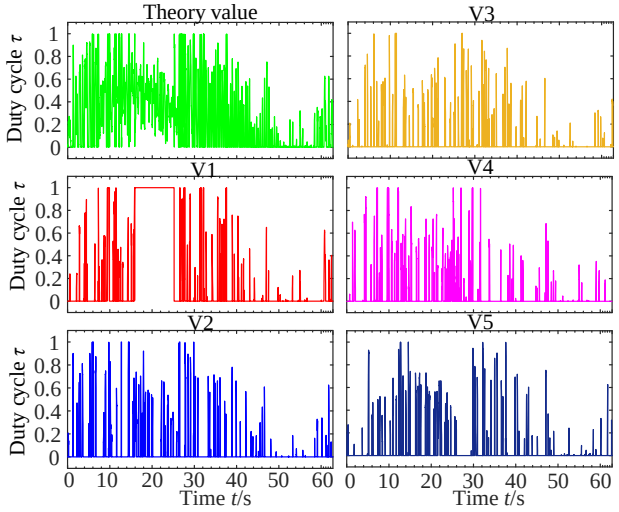

a) Duty cycles of each HSV and its theory value

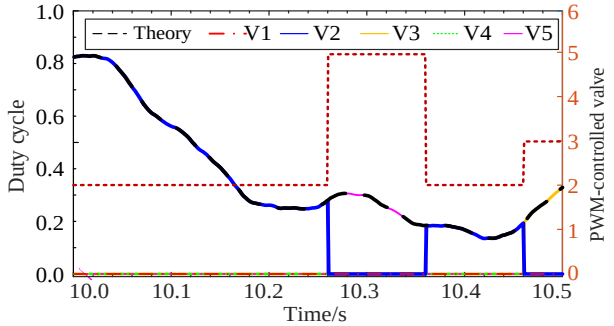

b) Partial magnification of duty cycles

Fig. 22. Duty cycle and its partial magnification at ω_1

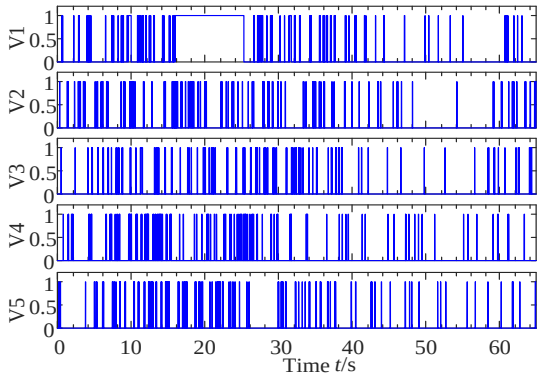

Fig. 23. Control signals of the DFCU-PA at ω_1

In comparison to the non-uniform switching control strategy, the switching numbers under PWM control are evenly distributed from a single valve to each valve, which is beneficial to ensuring the average life and reliability of the DFCU and its system. The signals of the PNM-controlled valves are also randomly assigned and given to the corresponding HSV. At the same time, each HSV provides its own signals to the cost function for the calculation of the signals at the next cycle.

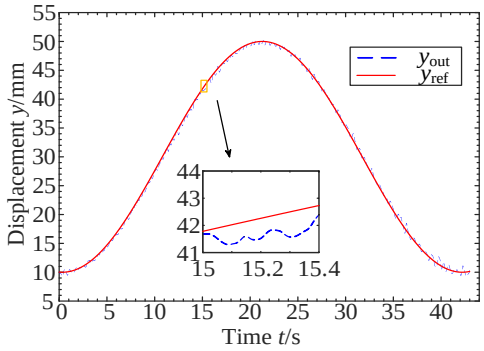

Fig. 24. Displacement curves at ω_2

Similarly, the experimental results of equivalent continuous metering control with uniform switching strategy at ω_2 are shown in Figure 24-25. The position control accuracy is slightly better than that of the non-uniform switching strategy, with the average position error is about 0.338 mm. The quality factor is about 0.065 s for the maximum position error 1.330 mm to the maximum velocity 20.46 mm/s. Figure 25 obviously shows that each valve distributes more evenly distributed than that of the non-uniform switching strategy. During 15.5-16 s in its partial magnification, the theoretical duty cycle distributes from V4→V1→V5→V4→V2. The duty cycle is randomly assigned to a HSV every 100ms using uniformly distributed random permutations for DFCUs. At the same time, the signal of each HSV is fed back to the cost function for the calculation of the next cycle. The signals of the PNM-controlled valves are then assigned at random.

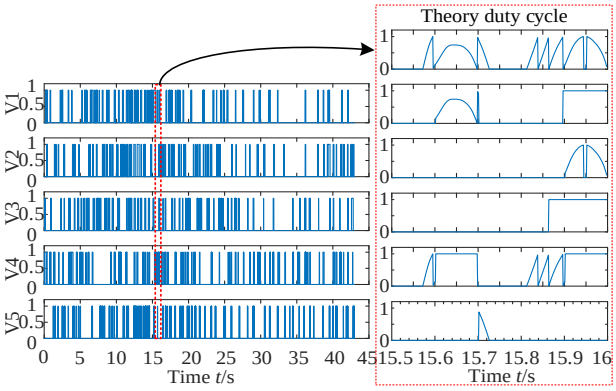

Fig. 25. Control signals of DFCU-PA at ω_2

The comparison indicators under different control strategies and frequencies are summarized in Table IV.

TABLE IV RESULTS OF DIFFERENT STRATEGIES

Indicators	Non-uniform switching		Uniform switching	
	ω_1	ω_2	ω_1	ω_2
μ a)	0.236 mm	0.406 mm	0.215 mm	0.338 mm
e_{max} b)	0.831 mm	1.590 mm	0.830 mm	1.330 mm
σ c)	0.161 mm	0.295 mm	0.187 mm	0.250 mm
ρ	0.128 s	0.112 s	0.140 s	0.065 s

a) Average error; b) Maximum error; c) Standard deviation

Therefore, the switching numbers for each valve with or without uniform switching distribution are counted in Table V.

TABLE V UNIFORMITY FOR DIFFERENT STRATEGIES

Switching Number (S)	Non-uniform switching		Uniform switching	
	ω_1	ω_2	ω_1	ω_2
V1	1125	908	218	260
V2	145	178	245	298
V3	2	78	226	268
V4	0	18	254	286
V5	0	0	232	360
Total	1273	1182	1177	1472
D	20.0%	38.3%	80.0%	79.7%

From the statistical results in Table V, the dispersion indexes D are 20% at ω_1 and 38.3% at ω_2 without a uniform switching strategy, while using the uniform switching strategy, the dispersion indexes D are 80% and 79.7% at ω_1 and ω_2, respectively. Results show that the switching numbers of each valve can be distributed more evenly almost without compromising the accuracy of the displacement control.

V. CONCLUSION

In this study, the equivalent spool displacement is defined for DFCUs based on the opening number of PNM-controlled valves and the duty cycle of the PWM-controlled valve to replace multiple discrete variables, which is simple but practical. Then, a model-free equivalent continuous metering control for an EDVS based on the equivalent spool displacement was presented. The feasibility of the equivalent continuous metering control method is validated by simulation and experiment. On this basis, the uniform switching control based on uniformly distributed random permutations for DFCUs, and the PNM control based on cost function are proposed for high reliability. The proposed control algorithm not only provides a similar control accuracy compared to the non-uniform switching strategy but optimizes the distribution of switching numbers of each valve. The simulation and experimental results demonstrated that the equivalent continuous metering control with uniform switching strategy makes the switching numbers of each valve more uniform and improves the overall reliability of the EDVS.

Only the feasibility and effectiveness of the proposed model-free control from the viewpoint of control are discussed in this paper. In future work, the energy-saving control method in four working quadrants would be further investigated to make full use of the energy-saving advantages of digital hydraulics.

ACKNOWLEDGMENT

This work was supported by the National Natural Science Foundation of China (Grant No. 51975507) and the Innovation Funding for Postgraduates in Hebei Province (Grant No. CXZZBS2022141). No conflicts of interest and financial disclosures.

REFERENCES

[1] B. Xu, M. Cheng, "Motion control of multi-actuator hydraulic systems for mobile machineries: Recent advancements and future trends," *Front. Mech. Eng.*, vol. 13, no. 2, pp. 151-166, Nov. 2018, doi: 10.1007/s11465-018-0470-5.

[2] D. B. Roemer, M. M. Bech, P. Johansen and H. C. Pedersen, "Optimum Design of a Moving Coil Actuator for Fast-Switching Valves in Digital Hydraulic Pumps and Motors," *IEEE-Asme T. Mech.*, vol. 20, no. 6, pp. 2761-2770, Dec. 2015, doi: 10.1109/TMECH.2015.2410994.

[3] H. Y. Yang, S. Wang, B. Zhang, H. C. Hong and Q. Zhong, "Development and prospect of digital hydraulic valve and valve control system," *J. Jilin Uni. (Eng. Tec.)*, vol. 46, no. 5, pp. 1494-1505, Sep 2016.

[4] M. Linjama, "Digital fluid power: State of the art," in *Proc.* SICFP, Tampere, Finland, May, 2011, pp. 18-20.

[5] V. H. Donkov, T. Andersen, M. Linjama and M. Ebbesen, "Digital hydraulic technology for linear actuation: a state of the art review," *Int. J. Fluid Power*, vol. 21, no. 2, pp. 263-304, Dec. 2020, doi:10.13052/ijfp1439-9776.2125

[6] Q. Zhang, X. Kong, B. Yu, Z. Jin and Y. Kang. "Review and development trend of digital hydraulic technology," *Appl. Sci.*, vol. 10, no. 2, pp. 579, Jan 2020, doi: 10.3390/app10020579.

[7] M. Pan and A. Plummer. "Digital switched hydraulics," *Front. Mech. Eng.*, vol. 13, no. 2, pp. 225-231, Feb. 2018, doi: 10.1007/s11465-018-0509-7.

[8] H. Tian, P. Y. Li and J. D. Van de Ven, "Valve timing control for a digital displacement hydraulic motor using an angle-domain repetitive controller," *IEEE-Asme T. Mech*, vol. 24, no. 3, pp. 1306-1315, June 2019, doi: 10.1109/TMECH.2019.2906347.

[9] M. Cai, Y. Wang, Z. Jiao and Y. Shi, "Review of fluid and control technology of hydraulic wind turbines," *Front. Mech. Eng.*, vol. 12, no. 3, pp. 312-320, May 2017, doi: 10.1007/s11465-017-0433-2.

[10] H. Liu, Y. Li, Y. Lin, J. Bao, W. Li and Y. Wang, "The application of the digital controlled hydraulic cylinders group in pendulum wave energy," *IEEE-Asme T. Mech.*, vol. 25, no. 2, pp. 673-682, Apr 2020, doi: 10.1109/TMECH.2019.2962206.

[11] Z. You, J. Gao, F. Chu and T. Shi, "Wind turbine dynamic modeling, condition monitoring and diagnosis," *Front. Mech. Eng.*, vol. 12, no. 3, pp. 279-280, Jul 2017, doi: 10.1007/s11465-017-0476-4.

[12] C. Yuan, A. Plummer and M. Pan, "Efficient control of a switched inertance hydraulic converter with a time-varying load," in *Proc. FPMC*, Virtual, Online, 2021, pp. FPMC2021-68832.

[13] C. Noergaard, E. L. Madsen, J. M. T. Joergensen, J. H. Christensen and M. M. Bech, "Test of a novel moving magnet actuated seat valve for digital displacement fluid power machines," *IEEE-Asme T. Mech.*, vol. 23, no. 5, pp. 2229-2239, Oct. 2018, doi: 10.1109/TMECH.2018.2866914.

[14] N. H. Pedersen, P. Johansen and T. O. Andersen, "Feedback control of pulse-density-modulated digital displacement transmission using a continuous approximation," *IEEE-Asme T. Mech.*, vol. 25, no. 5, pp. 2472-

2482, Oct. 2020, doi: 10.1109/TMECH.2020.2980122.
[15]Y. Shang, R. Li, S. Wu, X. Liu, Y. Wang and Z. Jiao, "A research of high-precision pressure regulation algorithm based on on/off valves for aircraft braking system," *IEEE T. Ind. Electron.*, vol. 69, no. 8, pp. 7797-7806, Aug. 2022, doi: 10.1109/TIE.2021.3108705.
[16]A. Laamanen, L. Siivonen, M. Linjama and M. Vilenius, "Digital flow control unit-an alternative for a proportional valve?," in *Proc. PTMC*, Bath, UK, 2004, pp. 297-308.
[17]M. Linjama and M. Vilenius, "Digital hydraulics-towards perfect valve technology, " in *Proc. SICFP*, Tampere, Finland, May, 2007, pp. 21-23.
[18]A. Laamanen, M. Linjama and M. Vilenius, "On the pressure peak minimization in digital hydraulic," in *Proc. SICFP*, Tampere, Finland, May 21-23, 2007, pp. 107-121.
[19]C. Stauch, J. Rudolph and F. Schulz, "Some aspects of modelling, dimensioning, and control of digital flow control units," in *Proc. DFP*, Linz, Austria, 2015, pp. 101-113.
[20]S. Rudolf and W. Bernd, "Have mushrooms grown-the status and expected further development of digital fluid power," in *Proc. DFP*, Linz, Austria, September, 2011, pp. 5–9.
[21]A. Plöckinger, M. Huova and R. Scheidl, "Simulation and experimental results of PWM control for digital hydraulics," in *Proc. DFP*, Tampere, 2012, pp. 133.
[22]B. Zhang, Q. Zhong, Ma J, H. Hong, H. Bao, Y. Shi and H. Y. Yang, "Self-correcting PWM control for dynamic performance preservation in high speed on/off valve," *Mechatronics*, vol. 55, pp. 141-150, Sep 2018, doi: 10.1016/j.mechatronics.2018.09.001.
[23]Q. Gao, Y. C. Zhu, Z. Luo and N. Bruno, "Investigation on adaptive pulse width modulation control for high speed on off valve," *J. Mech. Sci. Technol.*, vol. 34, no. 4, pp.1711-1722, Apr 2020, doi: 10.1007/s12206-020-0333-y.
[24]Q. Gao, Y. C. Zhu, Z. Luo and X. Chen, "Analysis and optimization of compound PWM control strategy for high-speed on-off valve," *Acta Aeronautica et Astronautica Sinica.*, vol. 45, no. 6, pp. 1129-1136, 2019.
[25]C. Ferraresi, "A new PCM-PWM combined technique for pneumatic flow-regulation valves," in *Proc. JHBMC*, Budapest, 1994, pp. 385-390.
[26]G. Belforte, S. Mauro and G. Mattiazzo, "A method for increasing the dynamic performance of pneumatic servo systems with digital valves," *Mechatronics.*, vol. 14, no. 10, pp. 1105-1120, Dec 2004, doi: 10.1016/j.mechatronics.2004.06.006.
[27]M. Huova and A. Plockinger, "Improving resolution of digital hydraulic valve system by utilizing fast switching valves," in *Proc. DFP*, Tampere, Finland, 2010, pp. 79–92.
[28]M. Paloniitty and M. Linjama, "High-linear digital hydraulic valve control by an equal coded valve system and novel switching schemes," *P. I. Mech. Eng. I-J. Sys.*, vol. 232, no. 3, pp. 258-269, Jan. 2018, doi: 10.1177/0959651817750519.
[29]Q. Gao, M. Linjama, M. Paloniitty and Y. Zhu, "Investigation on positioning control strategy and switching optimization of an equal coded digital valve system," *P. I. Mech. Eng. I-J. Sys.*, vol. 234, no. 8, pp. 959-972, Nov 2020, doi: 10.1177/0959651819884749.
[30]T. Muto, H. Yamada and Y. Suematsu, "Digital control of hydraulic actuator system operated by differential pulse width modulation," *JSME Int. J.*, vol. 33, no. 4, pp. 641-648, Feb 2008, doi: 10.1299/jsmec1988.33.641.
[31]B. Juergen, "Safety in digital-hydraulics (EN ISO 13849)," in *Proc. DFP*, Linz, Austria, Sep, 2011, pp. 155–168.
[32]M. Linjama, M. Huova and M. Karvonen, "Modelling of flow characteristics of on/off valves," in *Proc. DFP*, Tampere, Finland, Oct. 24-25, 2012, pp. 1-14.
[33]J. Yao, P. Wang, Z. Dong, D. Jiang and T. Sha, "A novel architecture of electro-hydrostatic actuator with digital distribution," *Chin. J. Aeronaut.*, 2021, 34(5): 224-238.
[34]L. Siivonen, M. Linjama and M. Vilenius, "Accurate flow control with digital valve system," in *Proc. NCFP*, Las Vegas, USA, Mar. 12-14, 2008, pp. 287-294.
[35]M. Linjama, L. Siivonen and M. Huova. "Numerically efficient flow model for on/off valves", in *Proc. DFP*, Linz, Austria, Feb. 26–27, 2015, pp. 164-172.
[36]J. Mattila, J. Koivumäki, D. G. Caldwell and C. Semini, "A survey on control of hydraulic robotic manipulators with projection to future trends," *IEEE-Asme T. Mech*, vol. 22, no. 2, pp. 669-680, Apr. 2017, doi: 10.1109/TMECH.2017.2668604.
[37]W. Zhu, T. Lamarche, E. Dupuis, D. Jameux, P. Barnard and G. Liu, "Precision control of modular robot manipulators: The VDC approach with embedded FPGA," *IEEE T. Robot*, vol. 29, no. 5, pp. 1162-1179, Oct. 2013, doi: 10.1109/TRO.2013.22656.

Pei Wang was born in Hebei, China, in 1991. She received her M.S. degree in Mechanical Engineering from Yanshan University, Qinhuangdao, China, in 2018. She is currently working toward her Ph.D. research in Fluid Transmission and Control at Tampere University in Finland and the School of Mechanical Engineering, Yanshan University.

Her research interests include digital hydraulic system modeling, simulation and control, and fault diagnose and fault tolerant.

Yuwang Cheng was born in Hebei, China, in 1998. He received the B.S. degree in Mechanical Engineering from Yanshan University, Qinhuangdao, China, in 2020. He is currently working toward the M.S. degree in in mechatronics engineering in the School of Mechanical Engineering, Yanshan University, Qinhuangdao, China.

His research interests include digital hydraulic system modeling, simulation, and the energy-saving control method.

Matti Linjama obtained a Ph.D. degree at Tampere University of Technology, Finland in 1998.

Currently, he is an adjunct professor at the Faculty of Engineering and Natural Sciences, Tampere University. He started the study of digital hydraulics in 2000 and has focused on the topic since then. Currently, he is the leader of the digital hydraulics research group, and his professional interests include the study of hydraulic systems with high performance and energy efficiency.

Jing Yao received the Ph.D. degree in mechatronics engineering from Yanshan University, Qinhuangdao, China, in 2009.

From 2009 he was a Lecturer at Yanshan University, where he has been professor since 2017. She is currently the Associate Dean of the School of Mechanical Engineering at Yanshan university. Her research interests include hydraulic servo control, modeling and simulation, dynamics and control of digital hydraulic.

Dongsheng Shan received the Ph.D. degree in mechatronics engineering from Yanshan University, Qinhuangdao, China, in 2007.

From 2008 to 2011, he was a Postdoctoral Fellow at Tsinghua University. Currently, he is executive chairman at Ningbo Safe Brakes Systems Co., Ltd. His research interests include high speed on/off valves design and advanced brakes system control.